

Quantum Quenches in Isolated Quantum Glasses out of Equilibrium

S. J. Thomson^{1,2,*}, P. Urbani^{2,†} and M. Schiró^{3‡}

¹*Centre de Physique Théorique, CNRS, Institut Polytechnique de Paris, Route de Saclay, F-91128 Palaiseau, France*

²*Université Paris-Saclay, CNRS, CEA, Institut de physique théorique, 91191, Gif-sur-Yvette, France*

³*JEIP, USR 3573 CNRS, Collège de France, PSL University, 11, place Marcelin Berthelot, 75231 Paris Cedex 05, France*

 (Received 2 May 2019; revised 23 July 2020; accepted 19 August 2020; published 15 September 2020)

In this work, we address the question of how a closed quantum system thermalizes in the presence of a random external potential. By investigating the quench dynamics of the isolated quantum spherical p -spin model, a paradigmatic model of a mean-field glass, we aim to shed new light on this complex problem. Employing a closed-time Schwinger-Keldysh path integral formalism, we first initialize the system in a random, infinite-temperature configuration and allow it to equilibrate in contact with a thermal bath before switching off the bath and performing a quench. We find evidence that increasing the strength of either the interactions or the quantum fluctuations can act to lower the effective temperature of the isolated system and stabilize glassy behavior.

DOI: [10.1103/PhysRevLett.125.120602](https://doi.org/10.1103/PhysRevLett.125.120602)

Introduction.—Understanding how and why many-body systems can fail to reach thermal equilibrium is both of fundamental value, as it allows us to test the hypothesis underlying equilibrium statistical physics, and of practical interest. In fact systems which fail to equilibrate can often exhibit rich new dynamical phenomena not seen in typical thermal states [1–4]

Two main mechanisms of ergodicity breaking in many-body quantum systems have emerged recently. On the one hand, quantum integrable systems have an extensive number of conserved charges and so do not thermalize to a state whose macroscopic properties are determined by only a few quantities (such as energy and density) [5]. On the other hand, the interplay of disorder and interactions can give rise to a robust mechanism for ergodicity breaking, the many-body equivalent of Anderson localization, *a.k.a.* many body localization (MBL), which does not require fine tuning to (typically isolated) integrable points. The absence of thermalization in MBL is related to an *emergent* integrability [6–10].

In between those two limits, for which thermalization fails on all timescales, there is a huge class of systems for which thermalization is possible but only on very long timescales. These are glassy systems, whose dynamics display ergodicity breaking due to metastability. In this case, the dynamical evolution is trapped by exponentially many metastable states that forbid equilibration on short timescales. In finite dimensions, such metastable states have a finite (but very long) lifetime, while in the mean field limit their lifetime diverges with the system size (or dimension) due to the divergence of the free energy barriers between them. Nevertheless those systems are never completely out of equilibrium since in the end they relax

on timescales that scale exponentially in either the system size or dimension [11,12].

In contrast with MBL and integrable systems, glassy systems do not depend crucially on isolation from their environment and indeed most investigations on the dynamical behavior of quantum glasses have focused on a dissipative setting, where the system is coupled to a thermal bath. Here important progress has been achieved through the solution of simplified fully connected models [13–18]. An interesting question which has received far less attention concerns the dynamics of isolated quantum glasses. Recently, the properties of highly excited eigenstates of paradigmatic mean field models of quantum glasses and their resulting dynamics have been investigated numerically through exact diagonalization of finite size systems [19], analytically using forward scattering approximations [20–22], and more recently through a mapping to the Rosenzweig-Porter random matrix model [23]. Yet, in the thermodynamic limit the dynamical behavior of those quantum mean field models can be solved exactly using field theory techniques similar to those well developed for classical models [11].

In this work we extend those techniques to the quantum case, by focusing on the unitary dynamics of the isolated spherical quantum p -spin model, a paradigmatic example of a mean-field glass, whose Hamiltonian

$$\mathcal{H} = \frac{1}{2m} \sum_i \Pi_i^2 - \mathcal{J}(t) \sum_{i_1 < \dots < i_p} J_{i_1 \dots i_p} \sigma_{i_1} \dots \sigma_{i_p} \quad (1)$$

describes a set of spins σ_i all-to-all coupled by random p -body interactions $J_{i_1 \dots i_p}$ drawn from a Gaussian

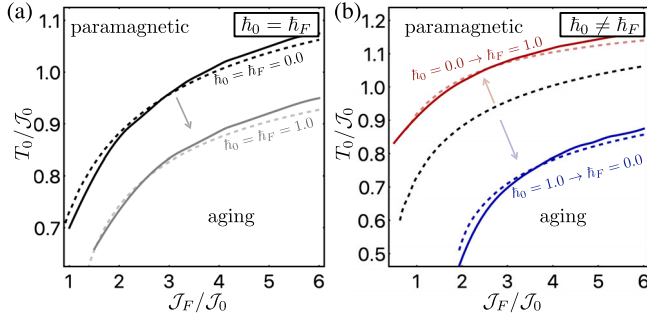


FIG. 1. Dynamical phase diagrams, as a function of initial temperature T_0 and strength of the interaction quench $\mathcal{J}_F/\mathcal{J}_0$, in two different scenarios. (a) (Left panel) The strength of quantum fluctuations is kept constant throughout the evolution, i.e., $\hbar_0 = \hbar_F$. In the classical case (top line) below a certain temperature the dynamics of the system displays aging. Finite quantum fluctuations suppress the aging regime (bottom line), as expected thermodynamically. (b) (Right panel) When the strength of quantum fluctuations is suddenly increased, $\hbar_F > \hbar_0$, the aging regime is enhanced (top curve) with respect to the classical phase diagram (dashed line). Vice versa, decreasing quantum fluctuations makes the aging regime shrink (bottom curve). Details of how the boundaries were obtained are given in the main text.

distribution with zero mean and unit variance. To make the model more tractable but still nontrivial, we treat the spins as continuous variables [24] and enforce the spherical constraint $\sum_i^N \sigma_i^2 = N$ by adding a Lagrange multiplier (hereafter denoted z). We further add a conjugate momentum Π_i where $[\Pi_i, \sigma_j] = i\hbar(t)\delta_{ij}$ are canonical commutation relations, and we allow $\hbar(t)$ to be time dependent in order to be able to change the strength of quantum fluctuations—for details, see the Supplemental Material [25]. This model has been extensively studied in both its classical [11,34–40] and quantum version, when coupled to a thermal bath [13–15,17,42–44]. At low temperature it displays a *dynamical* glass transition at a temperature T_d due to the emergence of long-lived glassy states. Below this tempera-

ture equilibration is never reached and the system ages forever (but not on exponential timescales). The dynamical temperature is a decreasing function of the strength of quantum fluctuations, as one may expect [14]. Though the isolated dynamics of the quantum p -spin model have not previously been studied, the classical isolated dynamics was recently investigated in Ref. [45]. Here we study the *quantum* evolution of this model: we prepare the system at some temperature T_0 in the paramagnetic phase and then we suddenly change both the strength of random couplings $\mathcal{J}(t)$ and the strength of quantum fluctuations measured by $\hbar(t)$, keeping the system isolated. The resulting nonequilibrium phase diagram, plotted in Fig. 1, features a high-temperature paramagnetic phase, where the system relaxes toward equilibrium, and a low-temperature phase where aging and breakdown of time-translational invariance

emerge. Surprisingly, we find that the phase boundary between the paramagnetic and aging regimes strongly depends on whether quantum fluctuations are kept constant (left panel) or suddenly changed (right panel) throughout the evolution. In the former case the aging regime shrinks with respect to its classical counterpart, as expected thermodynamically. In the latter, we find that a sudden increase of quantum fluctuations promotes rather than suppresses glassy effects (right panel, top curve), in striking contrast with the expectation based on the canonical equilibrium case of a system in contact with a finite temperature bath [13–15]. Such enhancement of aging effects is due to an interplay of quantum fluctuations and nonequilibrium effects. We interpret this intriguing result in terms of an effective temperature $T_{\text{eff}} < T_0$ for the isolated disordered quantum system, which in the absence of an external thermal bath is able to cool itself down through quantum fluctuations, eventually crossing the glass transition.

Dynamical equations for correlation and response.—Throughout this work we will focus in particular on the dynamics of correlation and response functions, which are defined by

$$C(t, t') = \frac{1}{2} \langle [\sigma(t), \sigma(t')]_+ \rangle, \quad (2)$$

$$R(t, t') = \theta(t - t') \frac{i}{\hbar(t')} \langle [\sigma(t), \sigma(t')]_- \rangle, \quad (3)$$

where $[A, B]_{\pm} = AB \pm BA$. The fully connected nature of the model defined in Eq. (1) allows us to derive closed dynamical equations that describe the evolution of correlation and response functions starting from an uncorrelated infinite temperature initial state. After disorder averaging and taking the $N \rightarrow \infty$ limit, the equations of motion for the correlation and response functions can be obtained following the method of Ref. [42] and are given by

$$[m\partial_t^2 + z(t)]R(t, t') = \delta(t - t') + \int_0^\infty dt'' \Sigma(t, t'')R(t'', t), \quad (4)$$

$$[m\partial_t^2 + z(t)]C(t, t') = \int_0^\infty dt'' \Sigma(t, t'')C(t'', t') + \int_0^{t'} dt'' D(t, t'')R(t', t''), \quad (5)$$

where we have defined the self-energies $\Sigma(t, t')$ and $D(t, t')$ as

$$\Sigma(t, t') = -\frac{p\mathcal{J}(t)\mathcal{J}(t')}{\hbar(t')} \text{Im} \left[C(t, t') - \frac{i\hbar(t')}{2} R(t, t') \right]^{p-1} \quad (6)$$

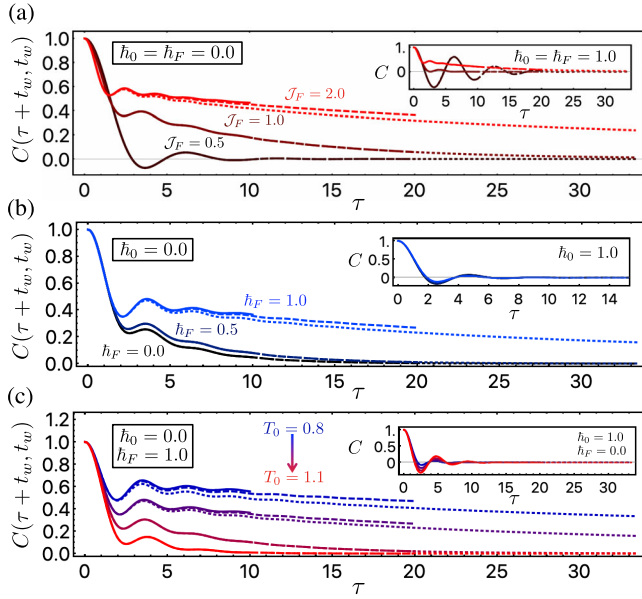


FIG. 2. Correlation functions after the second quench for a variety of different parameters, with $N = 15000$ steps, $t_{\max} = 100$ and $t_q = t_{\max}/2$. In each case, $\mathcal{J}_0 = 1.0$ and the wait times are $t_w = 16.67$ (dotted), $t_w = 30$ (dashed), and $t_w = 40$ (solid). (a) Quench of \mathcal{J} in the classical (main panel) and quantum (inset) model, at $T_0 = 0.8$. Quenches with $\mathcal{J}_F < \mathcal{J}_0$ pump energy into the system, while quenches with $\mathcal{J}_F > \mathcal{J}_0$ extract energy and can lead to aging behavior. (b) Quench of quantum fluctuations, for $T_0 = 0.9$ and $\mathcal{J}_F = 1$. A plateau emerges as \hbar_F is increased starting from the classical limit. Vice versa, decreasing quantum fluctuations make the system thermalize rapidly (inset). (c) Role of initial temperature, for $\mathcal{J}_F = \mathcal{J}_0 = 1$ and a sudden increase (main panel) or decrease (inset) of quantum fluctuations. In the first case lowering the temperature leads to a dynamical glass transition, consistent with the shifted phase boundary of Fig. 1(b).

$$D(t, t') = \frac{p\mathcal{J}(t)\mathcal{J}(t')}{2} \times \text{Re} \left[C(t, t') - \frac{i}{2} [\hbar(t')R(t, t') + \hbar(t)R(t', t)] \right]^{p-1}. \quad (7)$$

With respect to the classical dynamical equations [45], Eqs. (6)–(7) have extra self-energy contributions proportional to $\hbar(t)$ which arise from purely quantum fluctuations [13]. We perform the dynamical evolution subject to a time-dependent Lagrange multiplier $z(t)$ used to enforce the global spherical constraint. We can derive the dynamical equation for this by taking the equal-time limit of Eq. (5) to obtain [42]

$$z(t) = \int_0^t dt'' [\Sigma(t, t'')C(t'', t) + D(t, t'')R(t, t'')] - m\partial_t^2 C(t, t')|_{t' \rightarrow t^-}. \quad (8)$$

Equations (4), (5), and (8) are the three dynamical equations whose solution we will discuss in the rest of the Letter. Their causal structure allows for a simple discretization and numerical solution; for further details, see the Supplemental Material [25].

Finite temperature initial state preparation and double quench.—The dynamical equations [(4), (5), and (8)] describe the evolution of the system from an initial infinite temperature initial state uncorrelated with the disorder. Here we are instead interested in studying dynamics from an initial finite temperature state, which would, in principle, require a three branch Keldysh contour structure as recently discussed [46]. We instead perform the initial thermalization numerically through a double-quench protocol. Specifically, we first quench from infinite temperature to some $T_0 > T_d$ (where T_d is the equilibrium dynamical temperature of the spin glass transition) and $\mathcal{J}(0 < t < t_q) \equiv \mathcal{J}_0 = 1$ and $\hbar(0 < t < t_q) \equiv \hbar_0$ and allow the system to thermalize in contact with a thermal bath, which we assume to be a set of harmonic oscillators in thermal equilibrium at some temperature T_0 , as in Ref. [13]. This results in modified self-energies $\tilde{\Sigma}(t, t')$ and $\tilde{D}(t, t')$ in Eq. (7) due to the bath coupling, whose explicit expressions are given in Ref. [25]. Then, for $t \geq t_q$ we switch off the coupling to the bath and let the system evolve unitarily with $\mathcal{J}(t \geq t_q) \equiv \mathcal{J}_F$ and $\hbar(t \geq t_q) \equiv \hbar_F$. All temperatures are measured in units of \mathcal{J}_0 . Supporting data demonstrating that our system is well equilibrated to the bath temperature are shown in the Supplemental Material [25].

Results.—For concreteness we will set $p = 3$, though we expect our results to hold for any $p > 2$. In Fig. 2 we plot the dynamics of correlation function $C(\tau + t_w, t_w)$ at fixed $\mathcal{J}_0 = 1$ for different types of quenches. We first study the dynamics keeping fixed the strength of quantum fluctuations while quenching \mathcal{J} [panel (a)]. We see that increasing $\mathcal{J}_F > \mathcal{J}_0$ results in a slowdown of the dynamics and a plateau in the correlation function begins to emerge. Such a plateau is associated with a nonzero Edwards-Anderson glassy order parameter. In the classical case $\hbar_F = \hbar_0 = 0$ we therefore recover the results of Ref. [45], while in the quantum case $\hbar_F = \hbar_0 = 1$ (see inset) we see that similar quenches of \mathcal{J} do not lead to a well-formed plateau, indicating that the quantum aging boundary shifts toward larger values of $\mathcal{J}_F/\mathcal{J}_0$. This is consistent with the naive expectation that quantum fluctuations suppress aging behavior. The resulting phase diagram is shown in Fig. 1(a). A rather different picture emerges instead when quantum fluctuations are suddenly quenched rather than kept fixed, as we show in Fig. 2(b). Keeping the interaction fixed, $\mathcal{J}_F = \mathcal{J}_0$, and increasing the quantum fluctuations (main panel) strongly enhances the aging behavior of the system, as shown by the formation of a plateau and a waiting time dependence. On the contrary, reducing the value of $\hbar_F < \hbar_0$ leads to a rapid relaxation (inset). This surprising outcome for a quench of \hbar is further highlighted

in panel (c), where the dynamics for different initial temperature T_0 is studied. In particular we see that for an increase of \hbar (main panel) the system upon cooling crosses a dynamical glass transition, even in absence of an interaction quench ($\mathcal{J}_F = \mathcal{J}_0$), and for temperature well above the classical T_d . On the contrary, decreasing \hbar always keep the system in the paramagnetic phase. Those results therefore suggest that the aging regime is increased when quantum fluctuations are suddenly switched on, as we summarize in Fig. 1(b).

We remark that for the timescales accessible to our current simulations, the correlation function still decays and does not display a true plateau: this is likely an effect of not being able to access sufficiently long waiting times t_w to see the true plateau, as evidenced by the strengthening of the plateau for larger t_w . By approximating $C(\tau + t_w, t_w)|_{\tau \rightarrow \infty}$ by the value of the correlation function at the longest times accessible to our simulation, and identifying this value with the Edwards-Anderson order parameter q_{EA} , we can plot an approximate nonequilibrium phase diagram for the isolated quantum system, shown in Fig. 1. Within our simulation times, as clearly shown by Fig. 2, we cannot reach the true $t \rightarrow \infty$ value of q_{EA} . Instead, we can set a threshold value and approximate that all $q \leq q_{th}$ are slowly decaying paramagnetic solutions, whereas for $q > q_{th}$ the system is in a true glassy phase. The results of this are shown in the phase diagram in Fig. 1 by dashed lines, using $q_{th} \approx 0.2$, though the qualitative shape of the phase diagram does not depend strongly on this choice [47].

Effective temperature and quench-induced cooling.—The results presented above indicate that quantum fluctuations and nonequilibrium effects can strongly enhance glassiness and increase the region of parameters where aging effects are observed. This is surprising at first, since glassiness is a low temperature property, while exciting the system with a global quantum quench injects extensive energy and should intuitively induce heating [48,49]. We can understand this effect in terms of an effective thermalization of the isolated system to an effective temperature T_{eff} , as we show in detail by looking at the fluctuation-dissipation theorem (FDT) in the long-time regime of the dynamical equations for correlation and response [25]. In Fig. 3 we show that the T_{eff} extracted from FDT *decreases* with \hbar_F and eventually reaches the dynamical critical temperature T_d for the glass transition, below which the system fails to thermalize. By extracting the local minimum of T_{eff} from Fig. 3 and identifying it with the transition in our numerical data, we can draw a phase boundary with no free parameters, shown in Fig. 1 by the solid lines. Interestingly, the same effect of cooling by quantum fluctuations emerges from basic energetic arguments: indeed the effective temperature can be also estimated by comparing the postquench energy E_Q , which is conserved during the unitary evolution, to the equilibrium

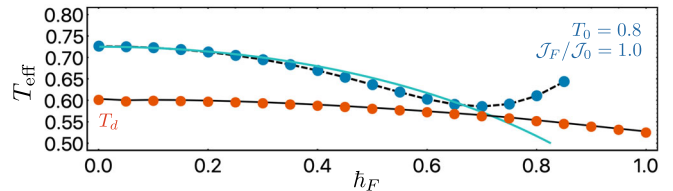


FIG. 3. Effective temperature T_{eff} after the second quench for a system initially equilibrated at $T_0 = 0.8$, $\mathcal{J}_F = \mathcal{J}_0 = 1.0$, and $\hbar_0 = 0$, obtained from the dynamical equation and the fluctuation-dissipation relation (blue points). As the strength of quantum fluctuations is increased, T_{eff} decreases until it reaches approximately the dynamical temperature T_d (red points, obtained from dynamical simulations in the presence of a thermal bath), here at a value $\hbar_F \approx 0.7$. Beyond this, T_{eff} displays the same nonmonotonic behavior seen in Ref. [45], indicating a violation of FDT and suggesting that the system has entered the glass phase. For comparison, the *thermodynamic* estimate for T_{eff} (see main text) is shown as a light blue line and matches almost perfectly the dynamical one. Other parameters $N = 15000$ and $t_{\text{max}} = 100$, with $t_q = t_{\text{max}}/2$.

internal energy of the system at a given value of \hbar_F , i.e., $E_Q = U(T_{\text{eff}}, \hbar_F)$. Solving this equation for our model in the static approximation [14,25], which is valid in the high temperature phase under consideration, we obtain a *thermodynamic* estimate for T_{eff} which almost perfectly matches the dynamical one obtained from FDT in the regime where the system thermalizes (see light blue line in Fig. 3).

Discussion.—In our specific model (1) the strength of quantum fluctuations is controlled by the magnitude of \hbar . A natural question concerns whether the qualitative picture we presented so far would change in more realistic situations where quantum fluctuations are controlled by the action of a transverse field Γ , such as in the Ising p -spin quantum glass [50–53]. In thermal equilibrium it is known that the spherical and the Ising p -spin share much of their physics [14,17,54,55], including the phase diagram that features a quantum glass to paramagnet phase transition driven by the strength of quantum fluctuations, encoded, respectively, in \hbar or Γ . Whether this analogy remains valid also for the out of equilibrium dynamics is *a priori* not obvious. Using energetic arguments [25] we estimate the effective temperature in the Ising p -spin after a quantum quench of the transverse field and show that, indeed, this quantity shows the same qualitative behavior in the two models. In particular we show that also in the Ising p -spin an increase of quantum fluctuation (i.e., a quench to a larger value of Γ) can lead to a decrease of the effective temperature, i.e., a cooling through quantum fluctuations that appears therefore a robust feature of isolated quantum glasses. This result is also of practical relevance, since quantum simulation of Ising p -spin models can be realized using arrays of superconducting qubits, which are modeled as two level systems with random Ising couplings and transverse fields, the latter tunable in real time and therefore

amenable to sudden or slow quenches. In fact, these protocols are routinely explored in the field of quantum annealing [56]. Superconducting qubits also offer enough flexibility in fabrication and design such that arranging effective multispin interactions, such as those relevant for our p spin with $p > 2$, has indeed been already reported [57,58].

Conclusions.—In this work we have studied the quench dynamics of an isolated quantum glass. Remarkably, we have shown that suddenly increasing the strength of quantum fluctuations enhances aging behavior, in contradiction with common expectations based on the physics of quantum glasses coupled to the thermal environment. The key feature of this effect relies on a “cooling by quantum fluctuations” effect that we have shown to hold also for the more realistic Ising p -spin case, a model which can be quantum simulated using superconducting qubits.

Interesting future directions include starting from a low temperature glass phase at $T < T_d$, for which the corresponding dynamical equations are already available in Ref. [46], to see how the quantum glasses respond to nonequilibrium perturbations as well as to study the effect of a smooth quench protocol with finite duration, which may connect our results with investigations on quantum annealing done on related quantum glass models [53,59]. Solving the full real-time dynamics for other mean field models of isolated quantum glasses, such as the Ising p spin and the quantum Random Energy Model, using similar techniques would also be an interesting direction to take.

We acknowledge helpful discussions with D. Abanin, G. Biroli, L. Cugliandolo, and M. Tarzia. This work was supported by the grant Investissements d’Avenir from Laboratoire d’excellence Physique Atomes Lumière Matière (Labex PALM) (ANR-10-LABX-0039-PALM), the grant Dynamics of Disordered Quantum Systems from Domaine D’Intérêt Majeur Science Et Ingénierie En Région Île-De-France Pour Les Technologies Quantiques (DIM SIRTEQ) and by the CNRS through the PICS-USA-14750. The majority of the computations were performed on the Collège de France Institut de Physique cluster computer.

*steven.thomson@polytechnique.edu

†pierfrancesco.urbani@ipht.fr

*marco.schiro@ipht.fr

On leave from: Institut de Physique Théorique, Université Paris Saclay, CNRS, CEA, F-91191 Gif-sur-Yvette, France.

- [1] T. Kinoshita, T. Wenger, and D. S. Weiss, *Nature (London)* **440**, 900 (2006).
 [2] M. Gring, M. Kuhnert, T. Langen, T. Kitagawa, B. Rauer, M. Schreitl, I. Mazets, D. A. Smith, E. Demler, and J. Schmiedmayer, *Science* **337**, 1318 (2012).

- [3] D. Fausti, R. I. Tobey, N. Dean, S. Kaiser, A. Dienst, M. C. Hoffmann, S. Pyon, T. Takayama, H. Takagi, and A. Cavalleri, *Science* **331**, 189 (2011).
 [4] M. Mitrano, A. Cantaluppi, D. Nicoletti, S. Kaiser, A. Perucchi, S. Lupi, P. Di Pietro, D. Pontiroli, M. Riccò, S. R. Clark *et al.*, *Nature (London)* **530**, 461 (2016).
 [5] F. H. Essler and M. Fagotti, *J. Stat. Mech.* (2016) 064002.
 [6] M. Serbyn, Z. Papić, and D. A. Abanin, *Phys. Rev. Lett.* **111**, 127201 (2013).
 [7] D. A. Huse, R. Nandkishore, and V. Oganesyan, *Phys. Rev. B* **90**, 174202 (2014).
 [8] V. Ros, M. Müller, and A. Scardicchio, *Nucl. Phys.* **B891**, 420 (2015).
 [9] C. Monthus, *J. Stat. Mech.* (2016) 033101.
 [10] S. J. Thomson and M. Schiró, *Phys. Rev. B* **97**, 060201(R) (2018).
 [11] T. Castellani and A. Cavagna, *J. Stat. Mech.* (2005) P05012.
 [12] A. Cavagna, *Phys. Rep.* **476**, 51 (2009).
 [13] L. F. Cugliandolo and G. Lozano, *Phys. Rev. B* **59**, 915 (1999).
 [14] L. F. Cugliandolo, D. R. Grepel, and C. A. da Silva Santos, *Phys. Rev. B* **64**, 014403 (2001).
 [15] L. F. Cugliandolo, D. R. Grepel, G. Lozano, H. Lozza, and C. A. da Silva Santos, *Phys. Rev. B* **66**, 014444 (2002).
 [16] G. Biroli and O. Parcollet, *Phys. Rev. B* **65**, 094414 (2002).
 [17] L. F. Cugliandolo, D. R. Grepel, G. Lozano, and H. Lozza, *Phys. Rev. B* **70**, 024422 (2004).
 [18] T. E. Markland, J. A. Morrone, B. J. Berne, K. Miyazaki, E. Rabani, and D. R. Reichman, *Nat. Phys.* **7**, 134 (2011).
 [19] C. R. Laumann, A. Pal, and A. Scardicchio, *Phys. Rev. Lett.* **113**, 200405 (2014).
 [20] C. L. Baldwin, C. R. Laumann, A. Pal, and A. Scardicchio, *Phys. Rev. B* **93**, 024202 (2016).
 [21] C. L. Baldwin, C. R. Laumann, A. Pal, and A. Scardicchio, *Phys. Rev. Lett.* **118**, 127201 (2017).
 [22] C. L. Baldwin and C. R. Laumann, *Phys. Rev. B* **97**, 224201 (2018).
 [23] L. Faoro, M. V. Feigelman, and L. Ioffe, *Ann. Phys. (Amsterdam)* **409**, 167916 (2019).
 [24] J. M. Kosterlitz, D. J. Thouless, and R. C. Jones, *Phys. Rev. Lett.* **36**, 1217 (1976).
 [25] See Supplemental Material at <http://link.aps.org/supplemental/10.1103/PhysRevLett.125.120602> for technical details about the derivation and numerical solution of dynamical equations, additional data on effective equilibration and effective temperature analysis of the Ising p -spin model, which also includes Refs. [26–33].
 [26] A. J. Bray and M. A. Moore, *J. Phys. C* **13**, L655 (1980).
 [27] A. Georges, G. Kotliar, W. Krauth, and M. J. Rozenberg, *Rev. Mod. Phys.* **68**, 13 (1996).
 [28] Y. Y. Goldschmidt and P.-Y. Lai, *Phys. Rev. Lett.* **64**, 2467 (1990).
 [29] J. Miller and D. A. Huse, *Phys. Rev. Lett.* **70**, 3147 (1993).
 [30] J. V. Alvarez and F. Ritort, *J. Phys. A* **29**, 7355 (1996).
 [31] F. Ritort, *Phys. Rev. B* **55**, 14096 (1997).
 [32] M. J. Rozenberg and D. R. Grepel, *Phys. Rev. Lett.* **81**, 2550 (1998).
 [33] K. Takahashi, *Phys. Rev. B* **76**, 184422 (2007).
 [34] B. Derrida, *Phys. Rev. Lett.* **45**, 79 (1980).
 [35] B. Derrida, *Phys. Rev. B* **24**, 2613 (1981).

- [36] D. Gross and M. Mezard, *Nucl. Phys.* **B240**, 431 (1984).
- [37] T. R. Kirkpatrick and D. Thirumalai, *Phys. Rev. Lett.* **58**, 2091 (1987).
- [38] T. R. Kirkpatrick and D. Thirumalai, *Phys. Rev. B* **36**, 5388 (1987).
- [39] A. Crisanti, H. Horner, and H. J. Sommers, *Z. Phys. B* **92**, 257 (1993).
- [40] L. F. Cugliandolo and J. Kurchan, *Phys. Rev. Lett.* **71**, 173 (1993).
- [41] T. Castellani and A. Cavagna, *J. Stat. Mech.* (2005) P05012.
- [42] L. F. Cugliandolo and G. Lozano, *Phys. Rev. Lett.* **80**, 4979 (1998).
- [43] G. Biroli and L. F. Cugliandolo, *Phys. Rev. B* **64**, 014206 (2001).
- [44] L. F. Cugliandolo, G. Lozano, and H. Lozza, *Eur. Phys. J. B* **41**, 87 (2004).
- [45] L. F. Cugliandolo, G. S. Lozano, and E. N. Nessi, *J. Stat. Mech.* (2017) 083301.
- [46] L. F. Cugliandolo, G. S. Lozano, and N. Nessi, *J. Stat. Mech.* (2019) 023301.
- [47] To extract the true phase boundary one would need to consider the relaxation time of the system as a function of the control parameters and try to fit its divergence; however, the timescales required to perform this analysis are longer than accessible with our numerical code.
- [48] A. Mitra and T. Giamarchi, *Phys. Rev. Lett.* **107**, 150602 (2011).
- [49] M. Schiró and A. Mitra, *Phys. Rev. Lett.* **112**, 246401 (2014).
- [50] Y. Y. Goldschmidt, *Phys. Rev. B* **41**, 4858 (1990).
- [51] V. Dobrosavljevic and D. Thirumalai, *J. Phys. A* **23**, L767 (1990).
- [52] T. Obuchi, H. Nishimori, and D. Sherrington, *J. Phys. Soc. Jpn.* **76**, 054002 (2007).
- [53] T. Jörg, F. Krzakala, J. Kurchan, and A. C. Maggs, *Phys. Rev. Lett.* **101**, 147204 (2008).
- [54] T. M. Nieuwenhuizen and F. Ritort, *Physica (Amsterdam)* **250A**, 8 (1998).
- [55] K. Takahashi and Y. Matsuda, *J. Phys. Conf. Ser.* **297**, 012021 (2011).
- [56] S. Boixo, T. F. Rønnow, S. V. Isakov, Z. Wang, D. Wecker, D. A. Lidar, J. M. Martinis, and M. Troyer, *Nat. Phys.* **10**, 218 (2014).
- [57] M. Schöndorf and F. K. Wilhelm, *Phys. Rev. Applied* **12**, 064026 (2019).
- [58] D. Melanson, A. J. Martinez, S. Bedkihal, and A. Lupascu, *arXiv:1909.02091*.
- [59] T. Jörg, F. Krzakala, J. Kurchan, A. C. Maggs, and J. Pujos, *Europhys. Lett.* **89**, 40004 (2010).